Journal of Materials Chemistry B

Accepted Manuscript

ROYAL SOCIETY OF CHEMISTRY

www.rsc.org/materialsB

Manuscript for ***J. Mater. Chem. B***

Photodynamic tumor therapy of nanoparticles with chlorin e6 sown in poly(ethylene glycol) forester

Dong Jin Lee [a], Yu Seok Youn [b], Eun Seong Lee [a,*]

[a] Department of Biotechnology, The Catholic University of Korea, 43-1 Yeokgok 2-dong, Wonmi-gu, Bucheon, Gyeonggi-do 420-743, Republic of Korea

[b] School of Pharmacy, Sungkyunkwan University, 300 Chonchon-dong, Jangan-ku, Suwon, Gyeonggi-do 440-746, Republic of Korea

* To whom correspondence should be addressed.

Tel: +82-2-2164-4921, Fax: +82-2-2164-4865

E-mail: eslee@catholic.ac.kr

Abstract

We developed novel photosensitizing drug-carrying nanoparticles with poly(ethylene glycol) (PEG) forester. In this study, chlorin e6 (Ce6, a model photosensitizing drug) was grafted to poly(L-lysine) [poly(Lys)] derivative containing multiple PEG segments and carboxylic acids at its pendant chain and 3,4-dihydroxyhydrocinnamic acid (DOHA) at one terminal site in its backbone. The conjugate was bound to the surface of gold nanoparticles (AuNP) as a result of non-covalent interaction between its DOHA moiety and AuNP. These nanoparticles enabled elevated singlet oxygen generation due to the dequenching event of Ce6 molecules shielded in PEG forester. This system resulted in highly improved *in vitro*/*in vivo* photodynamic tumor cell ablation over the nanoparticles without PEG forester. We believe that this system with PEG forester for photosensitizing drugs possesses great potential for tumor therapy.

Keywords: Chlorin e6, poly(ethylene glycol) forester, dequenching, photodynamic tumor therapy.

Introduction

Photodynamic therapy (PDT) is a promising treatment modality that has been extensively studied and employed for the treatment of various diseases including tumors because it is a non-invasive treatment with precise therapeutic performance for tumor tissues and minimal side effects for normal tissues.[1-5] However, most photosensitizers (PSs) for PDT have low tumor selectivity and high hydrophobicity.[6,7] In particular, the low quantum yield of singlet oxygen generation, resulting from auto-quenched state of hydrophobic PSs, eventually limits the use of such PSs for clinical application.[8,9] For successful PDT, it is essential to prevent the auto-quenching effect of hydrophobic PSs through physical/chemical modification of PSs. Notably, recent research efforts have been focused on creating nanoparticle systems bearing amphiphilic polymers and hydrophobic PSs to decrease the auto-quenching effect of PSs and to improve the efficacy of PDT.[8-10] For example, PSs have usually been anchored to the surface of nanoparticles or embedded in the core of nanoparticles.[11-15] However, these technological attempts have not always resulted in clinical success, owing primarily to unsatisfactory photo-activity of PSs and limited functionality of polymeric components.

In this study, we report a novel PS incorporation method in which PS is sown in the hydrophilic shell of the nanoparticle. Specifically, we utilize polyethylene glycol (PEG) forester to prevent the auto-quenching effect of chlorine e6 (Ce6, a model PS). It is known that PEG, one of the most popular polymers, has very low toxicity, excellent solubility in aqueous solutions, extremely low immunogenicity, and oxygen carrying capacity.[16,17] Moreover, PEG conjugation leads to decreased reticuloendothelial system uptake of nanoparticles, and prolongs their circulation time.[16,17] To prepare Ce6 sown in PEG forester, we first modified poly(L-lysine) [poly(Lys)], a backbone polymer, via coupling of

succinylated 3,4-dihydroxyhydrocinnamic acid (DOHA-NHS) to the terminal amino group of poly(N^{ε}-benzyloxycarbonyl-L-lysine) [poly(Lys-cbz)], and removal of remaining cbz moieties in DOHA-*b*-poly(Lys-cbz) using trifluoroacetic acid (TFA)/33% HBr in acetic acid. Next, we conjugated succinylated Ce6 (Ce6-NHS) and succinylated methoxy-poly(ethylene glycol) (mPEG-NHS) to the free pendant ε-amino groups of DOHA-*b*-poly(Lys) using *N,N'*-dicyclohexylcarbodiimide (DCC) and *N*-hydroxysuccinimide (NHS) (Fig. 1). The residual ε-amino groups of DOHA-*b*-poly(Lys-*g*-Ce6-*g*-mPEG) were again modified to carboxylic acid groups using succinic anhydride (SA), finally producing DOHA-*b*-poly(Lys-*g*-Ce6-*g*-mPEG-*g*-SA) (Fig. 1). As a result, Ce6 molecules grafted to the poly(Lys) backbone polymer were located between PEG segments (PEG forester) (Fig. 2a), possibly lowering the auto-quenching effect between Ce6 molecules. Subsequently, the sticky DOHA tail of DOHA-*b*-poly(Lys-*g*-Ce6-*g*-mPEG-*g*-SA) was simply bound to the surface of AuNP (particle size in diameter=10 nm) via noncovalent coordinate binding[5,10] (Fig. 2a). Here, AuNP was used as a as a nanoparticular model substrate[5], expecting the enhanced permeability and retention (EPR) effect[4] of nanoparticles for improving *in vivo* tumor uptake. We expect that this nanoparticle system with the PEG forester for Ce6 may facilitate successful delivery of photo-active Ce6 to tumor site for efficient tumor ablation. In particular, the PEG forester will decrease the auto-quenching effect of hydrophobic Ce6 molecules and enhance the phototoxicity of Ce6 under light illumination.

Materials and methods

Materials

N^{ε}-benzyloxycarbonyl-L-lysine, triphosgene, anhydrous 1,4-dioxane, n-hexane, hexylamine, anhydrous dimethylformamide (DMF), anhydrous diethyl ether, 3,4-

dihydroxyhydrocinnamic acid (DOHA), *N,N'*-dicyclohexylcarbodiimide (DCC), *N*-hydroxysuccinimide (NHS), trifluoroacetic acid (TFA), 33% HBr in acetic acid, succinic anhydride, triethylamine (TEA), pyridine, dimethyl sulfoxide (DMSO), gold (III) chloride hydrate ($HAuCl_4$), sodium citrate, sodium hydroxide (NaOH), and 9,10-dimethylanthracene (DMA) were purchased from Sigma-Aldrich (USA). Chlorin e6 (Ce6) was obtained from Frontier Scientific Inc. (USA). RPMI-1640, fetal bovine serum (FBS), penicillin, trypsin, EDTA (Ethylenediaminetetraacetic acid), and streptomycin were purchased from Welgene Inc. (Korea). Succinylated mPEG (mPEG-NHS) was synthesized as described in detail in our previous reports.[18]

Synthesis of polymer conjugates

Poly(N^{ε}-benzyloxycarbonyl-L-lysine) [poly(Lys-cbz)], a backbone polypeptide, was prepared via ring-opening polymerization of *N*-carboxy-(N^{ε}-benzyloxycarbonyl)-L-lysine anhydride (9 mmol) (recrystallized in excess n-hexane after the chemical reaction of N^{ε}-benzyloxycarbonyl-L-lysine and triphosgene in anhydrous 1,4-dioxane at 50°C for 1 h) in the presence of hexylamine (as an initiator) (0.3 mmol) in anhydrous DMF (30 mL) at room temperature for 3 days, as described in our previous reports.[19] The resulting solution was recrystallized in excess diethyl ether, yielding poly(Lys-cbz). The terminal amine group of poly(Lys-cbz) (1 mmol) was coupled with succinylated DOHA (DOHA-NHS, 3 mmol) [prepared after the pre-activation of the carboxyl group of DOHA (3 mmol) using DCC (3.5 mmol) and NHS (3.5 mmol) in DMF] in DMF (30 mL) containing TEA (1 mL) at room temperature for 1 day. The solution was filtered and was lyophilized after adding excess anhydrous diethyl ether, resulting in the production of DOHA-*b*-poly(Lys-cbz) (hereafter termed 'P1', Table 1) (Fig. 1). Next, the benzyloxycarbonyl (cbz) groups of the resulting

polymer (Lys repeating unit 22.4, as determined from ^{1}H-NMR) were removed with TFA (5 mL)/33% HBr in acetic acid (5 mL) at room temperature for 30 min (Fig. 1). The resulting solution was recrystallized in excess ethanol/diethyl ether (50:50 vol.%), filtered and lyophilized. The yield of P1 was 91±4%, calculated after lyophilization.

Next, succinylated Ce6 (Ce6-NHS, 3 mmol) [prepared after the pre-activation of the carboxyl group of Ce6 (3 mmol) using DCC (1 mmol) and NHS (1 mmol)[20]] was grafted to P1 (0.6 mmol) in DMF (20 mL) containing TEA (1 mL) at room temperature for 1 day, yielding DOHA-*b*-poly(Lys-*g*-Ce6). The obtained DOHA-*b*-poly(Lys-*g*-Ce6) (0.2 mmol) was again reacted with mPEG-NHS (1 mmol) in DMF (20 mL) containing TEA (1 mL) at room temperature for 1 day, yielding DOHA-*b*-poly(Lys-*g*-Ce6-*g*-mPEG). Finally, DOHA-*b*-poly(Lys-*g*-Ce6) (0.2 mmol) or DOHA-*b*-poly(Lys-*g*-Ce6-*g*-mPEG) (0.2 mmol) were reacted with succinic anhydride (10 mmol) in DMSO (20 mL) containing TEA (1 mL) and pyridine (1 mL) at room temperature for 5 days, each yielding DOHA-*b*-poly(Lys-*g*-Ce6-*g*-succinic acid) [DOHA-*b*-poly(Lys-*g*-Ce6-*g*-SA)] (hereafter termed 'P3', Table 1) or DOHA-*b*-poly(Lys-*g*-Ce6-*g*-succinic acid-*g*-mPEG) [DOHA-*b*-poly(Lys-*g*-Ce6-*g*-mPEG-*g*-SA)] (hereafter termed 'P4', Table 1), respectively (Fig. 1). After the reaction was completed, the final solution was filtered and transferred to a pre-swollen dialysis membrane tube (Spectra/Por® MWCO 5K) and was dialyzed against fresh DMSO (for 2 days) and deionized water (for 2 days) to remove the non-reacted chemicals.[20] The solution was withdrawn from a dialysis membrane tube and was freeze-dried for 2 days. In addition, DOHA-*b*-poly(Lys-*g*-succinic acid) [DOHA-*b*-poly(Lys-*g*-SA)] (hereafter termed 'P2', Table 1) was synthesized as a control group with no photoactivity. The yields of P2, P3, and P4 were 84±2%, 73±3%, and 68±4%, respectively, calculated after lyophilization.

Characterization of the polymer conjugates

The chemical structure of the polymer conjugates (P1, P2, P3, and P4) was analyzed using a Bruker 300 MHz NMR Spectrometer (Bruker, Germany). The number average molecular weight (M_n) and weight average molecular weight (M_w) of the polymer conjugates were determined using a HPLC system (Waters, USA) equipped with a 410 differential refractometer and a gel permeation chromatography (GPC) KF-804 or GPC KF-805 column (Shodex, Tokyo, Japan) at a flow rate of 1.0 mL/min with DMF as the mobile phase at room temperature.[19]

AuNP preparation

To prepare AuNP, $HAuCl_4$ (2.5 mmol) was mixed with NaOH solution (7.7 mmol, 19.4 mL). The resulting solution was put into an oil bath at 110℃ for 30 min and then at 85°C for 10 min. Sodium citrate solution (166.7 mmol, 0.6 mL) was rapidly added into the solution under vigorous stirring.[21] The obtained solution was stirred for 10 min until the color was turned to wine red. Next, the synthesized polymer conjugate (P2, P3, and P4, 100 mg) was stirred with AuNP solution (10 mg) dispersed in deionized water (10 mL) at 25 ℃ for 8 h.[21] The concentration of each polymer conjugate bound to AuNP was calculated after measuring the weight of the dried precipitate (AuNP-P) after ultracentrifugation of the AuNP-P solution at 25000 rpm for 10 min.[22] The Ce6 concentration in AuNP-P was calculated by measuring the fluorescence intensity of free P3 or P4 remaining in the supernatant obtained after the ultracentrifugation of the AuNP-P solution (obtained immediately after the coupling reaction) at 25,000 rpm for 10 min.

Characterization of AuNP-P

The particle size distribution of each AuNP-P (0.1 mg/mL) dispersed in 150 mM

phosphate buffered saline (PBS, pH 7.4) was analyzed using a Zetasizer 3000 instrument (Malvern Instruments, USA) equipped with a He-Ne laser at a wavelength of 633 nm and a fixed scattering angle of 90°.[23] The morphology of each AuNP-P (10 μg/mL) was confirmed using a transmission electron microscope (TEM; JEM 1010, Japan).[22]

The zeta-potential of each AuNP-P (0.1 mg/mL, PBS, pH 7.4, 150 mM) was measured with a Zetasizer 3000 (Malvern Instruments, USA). Before the test, each sample was stabilized at room temperature for 4 h.[23]

In vitro photoactivity studies

The emission spectra of AuNP-P (equivalent Ce6 10 μg/mL) or free Ce6 (10 μg/mL) was measured using a Shimadzu RF-5301PC spectrofluorometer (USA) at λ_{ex} 405 nm and λ_{em} 600-800 nm.[24]

Generation of singlet oxygen from AuNP-P (equivalent Ce6 10 μg/mL) or free Ce6 (10 μg/mL) was confirmed using 9,10-dimethylanthracene (DMA).[23,24] DMA (20 mmol) was mixed with of AuNP-P (equivalent Ce6 10 μg/mL) or free Ce6 (10 μg/mL) in PBS (150 mM, pH 7.4). The solution was illuminated at a light intensity of 5.2 mW/cm^2 using a 670 nm laser source for 10 min. When the DMA fluorescence intensity (measured using a Shimadzu RF-5301PC spectrofluorometer at λ_{ex} 360 nm and λ_{em} 380-550 nm) reached a plateau after 1 h, the change in DMA fluorescence intensity (F_f - F_s) was plotted after subtracting each sample fluorescence intensity (F_s) from the full DMA fluorescence intensity (without Ce6, indicating no singlet oxygen, F_f).[20,23,24]

Cell culture

Human nasopharyngeal epidermal carcinoma KB cells (from the Korean Cell Line

Bank) were maintained in RPMI-1640 medium with 2 mM L-glutamine, 1 % penicillin-streptomycin, and 10 % FBS in a humidified standard incubator with a 5 % CO_2 atmosphere at 37℃. Prior to testing, cells (1×10^5 cells/mL), grown as a monolayer, were harvested by trypsinization using a 0.25 % (w/v) trypsin/0.03% (w/v) EDTA solution and seeded onto well plates containing RPMI-1640 medium.[20,23,24]

In vitro phototoxicity tests

Phototoxicity of AuNP-P with light illumination was tested for KB tumor cells.[23] Each AuNP-P or free Ce6 dispersed in RPMI-1640 medium were administered to cells plated in 96-well plates. The cells were incubated with each sample for 4 h and then washed three times with PBS (pH 7.4). The cells were illuminated at a light intensity of 5.2 mW/cm^2 using a 670 nm laser source for 10 min and then further incubated for 12 h. Cell viability was determined using a Cell Counting Kit-8 (CCK-8 assay).[20,23,24] In addition, a cell viability test of KB cells treated with each AuNP-P (10-100 μg/mL) without light illumination for 24 h was conducted to estimate the original toxicity of AuNP-P.

Animal care

In vivo studies were conducted with 6-week old female nude mice (BALB/c, nu/nu mice, Institute of Medical Science, Japan). Mice were maintained under the guidelines of an approved protocol from the Institutional Animal Care and Use Committee (IACUC) of the Catholic University of Korea (Republic of Korea).

In vivo uptake studies

To prepare *in vivo* xenografted tumors, KB tumor cells (1×10^7 cells in PBS pH 7.4) were

subcutaneously injected into female nude mice. When the tumor volume reached 50-100 mm^3, each AuNP (*i.v.* dose: equivalent Ce6 0.5 mg/kg) or free Ce6 (*i.v.* dose: 2.5 mg/kg) in PBS (150 mM, pH 7.4) was intravenously injected into the tumor-bearing nude mice through the tail vein. Fluorescence images were obtained at 1, 4, and 12 h post-injection using an Image Station 4000 MM (Kodak, USA) with a special C-mount lens and a long-wave emission filter (Omega Optical, Brattleboro, VT, USA).[23,24] In addition, the tumor tissues extracted (12 h post-injection) from the sacrificed nude mice were sliced using a microtome, and analyzed using an Image Station 4000 MM.[22]

***In vivo* photodynamic tumor therapy**

Each AuNP (*i.v.* dose: equivalent Ce6 0.5 mg/kg) or free Ce6 (*i.v.* dose: 2.5 mg/kg) in PBS (150 mM, pH 7.4) or only PBS (150 mM, pH 7.4, as a control) was intravenously injected into KB tumor-bearing nude mice through the tail vein. At 12 h post-injection, the tumor sites of the nude mice were locally illuminated for 40 min at a light intensity of 2.8 mW/cm^2 with a 670 nm laser source. The change in tumor volume was monitored over time. Tumor volume was calculated using the formula: tumor volume = length × $(width)^2/2$.[23,24] The relative tumor volume change (V/V_0), where V is the tumor volume at a given time and V_0 is the initial tumor volume, was plotted.

Statistical evaluation.

All of the results were analyzed via Student's t-test or ANOVA at a significance level of $p < 0.01$ (**). The MINITAB® *release 14* statistical software program was used for all statistical analyses.

Results and discussion

Nanoparticle preparation

In this study, we synthesized a poly(Lys) derivative containing multiple PEG segments and carboxylic acids at its pendant side groups and DOHA at one terminal site on its backbone. First, we prepared poly(Lys-cbz) {Lys repeating unit: 22.4, estimated based on the ^{1}H-NMR peaks using the integration ratio of the peaks at δ 0.90 [-C**H**$_3$, corresponding to the terminal group of poly(Lys)] and δ 4.25 [-C**H**-, corresponding to the repeating unit of poly(Lys)] (Fig. 2b)} after ring-opening polymerization of *N*-carboxy-(*N*$^{\varepsilon}$-benzyloxycarbonyl)-L-lysine anhydride as described in detail in our previous report.[19] One terminal primary amine of poly(Lys-cbz) was coupled with succinylated DOHA (DOHA-NHS) in DMF containing TEA, producing DOHA-*b*-poly(Lys-cbz). The cbz moieties of DOHA-*b*-poly(Lys-cbz) were detached using TFA/HBr. The obtained DOHA-*b*-poly(Lys) (P1, Table 1) showed apparent ^{1}H-NMR peaks at δ 6.25-6.75 (indicating the conjugation of DOHA) and no ^{1}H-NMR peaks at δ 7.0-7.5 (indicating the removal of cbz) (Fig. 2b). Next, P1 was reacted with succinylated Ce6 (Ce6-NHS) and succinylated mPEG (mPEG-NHS) in DMF containing TEA. The residual ε-amino groups of poly(Lys) were substituted to carboxylic acid groups after conjugating with succinic anhydride (SA), finally producing DOHA-*b*-poly(Lys-*g*-Ce6-*g*-mPEG-*g*-SA) (P4, Table 1). The degree of Ce6, mPEG, and SA substitution [defined as the number of each moiety (Ce6, mPEG, and SA) per repeating unit of poly(Lys)] in P4 were estimated based on the ^{1}H-NMR peaks using the integration ratio of the peaks at δ 0.90 [-C**H**$_3$, corresponding to the terminal group of poly(Lys)], δ 6.10 (-C**H**-, corresponding to the Ce6), δ 3.50 (-C**H**$_2$-, corresponding to the mPEG), and δ 2.40 (-CO-C**H**$_2$-, corresponding to the SA) (Fig. 2b). The degree of Ce6, mPEG, and SA substitution were 0.22, 0.19, and 0.52, respectively (Table 1). The M_n, M_w, and molecular weight

distribution (M_w/M_n) of P4 were 14.5 kDa, 27.7 kDa, and 1.91, respectively (Table 1). In addition, we synthesized DOHA-*b*-poly(Lys-*g*-SA) (P2, Table 1) and DOHA-*b*-poly(Lys-*g*-Ce6-*g*-SA) (P3, Table 1) as control groups. The degree of SA substitution in P2 was 0.81. The M_n, M_w, and molecular weight distribution (M_w/M_n) of P2 were 4.7 kDa, 7 kDa, and 1.49, respectively. The degree of Ce6 and SA substitution in P3 was 0.22 and 0.66, respectively. The M_n, M_w, and molecular weight distribution (M_w/M_n) of P3 were 7.1 kDa, 12.8 kDa, and 1.80, respectively (Table 1).

We prepared various combinations of AuNP using polymer conjugates (P2, P3, and P4) as listed in Table 2. The polymer conjugates (P2, P3, and P4) were non-covalently bound to the surface of AuNP in PBS.[10,21,22] We calculated the weight fractions of each polymer conjugate in AuNP-P after measuring the concentration of polymer conjugate remaining the supernatant obtained after ultracentrifugation of the AuNP-P solution at 25,000 rpm. On an averages, 13.7% P2, 10.8% P3, and 15.3% P4 (data not shown) were bound to the surface of AuNP as a result of noncovalent interaction between DOHA and AuNP (Fig. 2a). The Ce6 concentration in AuNP-P was also calculated by measuring the fluorescence intensity of Ce6-conjugated polymer (P3 and P4) remaining in the supernatant obtained after the ultracentrifugation of the AuNP-P solution. The weight fractions of Ce6 existing in AuNP-P were 21.8% (AuNP-P3) and 12.9% (AuNP-P4) (Table 2).

Physicochemical characteristics

The zeta-potential of AuNP-P2, AuNP-P3, and AuNP-P4 were -28.9±2.2, -31.9±0.8, and -16.5±1.6 mV, respectively (Table 2). It was thought that the nonionic mPEG conjugation increased the zeta-potential of AuNP-P. The images obtained from a transmission electron microscope (TEM) illustrate that each AuNP-P (average diameter of 51-75 nm, Table 2) was almost spherical (Fig. 3).

Photo-physical properties

To evaluate the photo-physical properties of AuNP-P, their light emission spectra (at λ_{ex} 405 nm and λ_{em} 600-800 nm) in PBS were investigated. The emission spectra of AuNP-P3, AuNP-P4, and free Ce6 showed distinct emission bands at 630-700 nm due to the presence of photo-responsive Ce6 molecules (Fig. 4a). Interestingly, AuNP-P4 exhibited strong light emission at 630-700 nm, probably due to the dequenching event of Ce6 molecules shielded in PEG forester.[20] However, AuNP-P3 (without PEG forester) showed low light emission at 630-700 nm, probably due to the auto-quenching event occurring between Ce6 molecules densely populated in one assembly nanoparticle.[8] In addition, AuNP-P2 (without Ce6) showed no emission band in the range of 600-800 nm. Next, we evaluated the photo-induced singlet oxygen generation from the nanoparticles in PBS under light illumination (5.2 mW/cm^2 at 670 nm for 10 min) (Fig. 4b). It is known that near infrared (NIR) light-absorbing Ce6 molecules can transfer the photon energy to oxygen dissolved in body fluid, thereby producing reactive oxygen species (*e.g.,* singlet oxygen) toxic to tumor cells.[20,23,24] As expected, AuNP-P4 in PBS exhibited highly increased singlet oxygen generation as a result of the dequenching event of Ce6 molecules[20] and the possible oxygen carrying capacity[16,17] of PEG. However, AuNP-P3 in PBS typically displayed decreased singlet oxygen generation, corresponding to the auto-quenching effect of Ce6 molecules. Free Ce6 in PBS showed less singlet oxygen generation (possibly due to the formation of its irregular hydrophobic aggregation in PBS) than AuNP-P4.[8,20]

***In vitro* phototoxicity**

Fig. 5a shows the *in vitro* phototoxicity of AuNP-P for KB tumor cells. Under light illumination (5.2 mW/cm^2 at 670 nm for 10 min), AuNP-P4 led to relatively higher levels of

tumor cell death at concentrations equivalent to Ce6 of 1-10 μg/mL. However, AuNP-P3 and free Ce6 exhibited less phototoxicity to tumor cells as a result of the down-regulated production of singlet oxygen. Prior to light illumination, AuNP-P3 and AuNP-P4 displayed negligible toxicity (Fig. 5b), indicating non-toxicity of the AuNP-P itself.

***In vivo* phototoxicity**

To ascertain the improved phototoxicity of AuNP-P4 in comparison with free Ce6 or AuNP-P3, we performed *in vivo* tumor inhibition test using KB tumor-bearing nude mice. First, we evaluated the *in vivo* tumor uptake of AuNP-P and free Ce6 using noninvasive photoluminescent imaging method.[20,23,24] At 12 h post-injection, the nude mice administered with AuNP-P4 (equivalent Ce6 0.5 mg/kg) allowed for high-resolution fluorescent images on the *in vivo* tumor site (Fig. 6a). A strong fluorescent Ce6 signal at the tumor site indicates high tumor uptake of AuNP-P4. This event may be originated from the enhanced permeability and retention (EPR) effect of nanoparticles that extravasated into tumor tissues *in vivo*, resulting in leading the preferential accumulation of AuNP-P4 in tumor tissues *in vivo*.[4,25-27] However, AuNP-P3 showed low fluorescent Ce6 signal at 12 h post-injection, probably due to the reduced fluorescent intensity of auto-quenched Ce6 molecules.[8] In addition, free Ce6 showed poor tumoral accumulation probably due to its nonspecific uptake in normal tissues and rapid clearance in body.[6,7] Furthermore, to verify the accumulation of AuNP-P4 in the interior tissue of the tumor, we sliced the *in vivo* tumor tissues using a microtome and observed the Ce6 fluorescence. Fig. 6b shows that AuNP-P4 efficiently infiltrated into the interior tumor tissue, which is comparable with the results obtained after treatment with free Ce6. Fig. 7 shows the *in vivo* therapeutic efficiency of AuNP-P and free Ce6 in the KB tumor-bearing nude mice model. At 12 h post-injection of each sample, solid tumors were locally illuminated at a light intensity of 2.8 mW/cm^2 using a 670 nm laser

source for 40 min, and then tumor volume regression were monitored daily for 7 days. Interestingly, significant regression in tumor volume was observed for the group treated with AuNP-P4. The relative tumor volume (V/V_0) of nude mice treated with AuNP-P4 was approximately 2.5 or 2.2 times smaller than those treated with AuNP-P3 or free Ce6 (Fig. 7a). Overall, AuNP-P4 was found to be more efficient for tumor regression when compared to free Ce6 and AuNP-P3 that exhibited a gradual increase in tumor volume (Fig. 7a & 7b). The vital behaviors of nude mice treated with AuNP-P or free Ce6 appeared equivalent to the non-treated nude mice and exhibited negligible change in their body weight, suggesting a negligible possibility of side effects (data not shown).

Conclusion

In this study, we synthesized a photosensitizing drug-conjugated poly(Lys) with multiple PEG segments and prepared nanoparticles stabilized using this polymer. In particular, a photosensitizing drug (Ce6) sown in multiple PEG segments (hydrophilic shell) of the nanoparticles showed highly increased singlet oxygen generation under light illumination. This property of nanoparticle enabled improved *in vivo* tumor ablation during photodynamic tumor treatment. Based on the results of this study, we anticipate that this system possesses great potential as an advanced technology platform for tumor treatment.

Acknowledgments

This work was financially supported by the Research Fund, 2015 of the Catholic University of Korea, by the GRRC program of Gyeonggi province [GRRC 2014-B01, Development of industrial nano-/micro-sized biomaterials for high performance drug release control], a grant from the National R&D Program for Cancer Control, Ministry for Health and Welfare,

Republic of Korea (No. 1320130), and a grant of the Korea Health Technology R&D Project through the Korea Health Industry Development Institute (KHIDI), funded by the Ministry of Health & Welfare, Republic of Korea (grant number: no HI14C1835).

References

1. B. Jang, J. Y. Park, C. H. Tung, I. H. Kim and Y. Choi, *ACS Nano*, 2011, **5**, 1086-1094.
2. T. J. Dougherty, C. J. Gomer, B. W. Henderson, G. Jori, D. Kessel, M. Korbelik, J. Moan and Q. Peng, *J. Natl. Cancer Inst.*, 1998, **90**, 889–905.
3. E. F. Gudgin Dickson, R. L. Goya and R. H. Pottier, *Cell. Mol. Biol.*, 2002, **48**, 939–954.
4. H. Maeda, *Ther. Deliv*., 2014, **5**, 627-630.
5. P. Dong, J. Xin, X. Yang, J. Jia, W. Wu and J. Li, *RSC Adv*., 2014, **4**, 44872–44878.
6. Z. Li, C. Wang, L. Cheng, H. Gong, S. Yin, Q. Gong, Y. Li and Z. Liu, *Biomaterials*, 2013, **34**, 9160-9170.
7. L. Cheng, C. Wang, L. Feng, K. Yang and Z. Liu, *Chem. Rev*., 2014, **114**, 10869-10939.
8. S. Wang, R. Gao, F. Zhou and M. Selke, *J. Mater. Chem.*, 2004, **14**, 487–493.
9. D. K. Chatterjee, L. S. Fong and Y. Zhang, *Adv. Drug Deliv. Rev.*, 2008, **60**, 1627–1637.
10. R. Baron, M. Zayats and I. Willner, *Anal. Chem*., 2005, **77**, 1566-1571.
11. R. Ideta, F. Tasaka, W. D. Jang, N. Nishiyama, G. D. Zhang, A. Harada, Y. Yanagi, Y. Tamaki, T. Aida and K. Kataoka, *Nano Lett*., 2005, **5**, 2426–2431.
12. W. D. Jang, N. Nishiyama, G. D. Zhang, A. Harada, D. L. Jiang, S. Kawauchi, Y. Morimoto, M. Kikuchi, H. Koyama, T. Aida and K. Kataoka, *Angew. Chem. Int. Ed.*, 2005, **117**, 423–427.
13. C. S. Lee, W. Park, S. J. Park and Kun Na, *Biomaterials*, 2013, **34**, 9227–9236.
14. D. S. Kwag, K. T. Oh and E. S. Lee, *J. Control. Release*, 2014, **187**, 83–90.
15. D. J. Lee, G. Y. Park, K. T. Oh, N. M. Oh, D. S. Kwag, Y. S. Youn, Y. T. Oh, J. W. Park and E. S. Lee, *Int. J. Pharm*., 2012, **434**, 257–263.
16. S. Zalipsky, *Adv. Drug Deliv. Rev.*, 1995, **16**, 157–182.
17. M. R. Hamblin, J. L. Miller, I. Rizvi, B. Ortel, E. V. Maytin and T. Hasan, *Cancer Res.*, 2001, **61**, 7155–7162.

18. N. M. Oh, K. T. Oh, Y. S. Youn, D. K. Lee, K. H. Cha, D. H. Lee and E. S. Lee, *Colloids Surf., B*, 2013, **101**, 298–306.

19. J. O. Lee, K. T. Oh, D. Kim and E. S. Lee, *J. Mater. Chem. B*, 2014, **2**, 6363-6370.

20. S. Y. Park, H. J. Baik, Y. T. Oh, K. T. Oh, Y. S. Youn and E. S. Lee, *Angew. Chem. Int. Ed.*, 2011, **50**, 1644–1647.

21. I. C. Sun, D. K. Eun, J. H. Na, S. Lee, I. J. Kim, I. C. Youn, C. Y. Ko, H. S. Kim, D. Lim, K. Choi, P. B. Messersmith, T. G. Park, S. Y. Kim, I. C. Kwon, K. Kim, and C. H. Ahn, *Chem. Eur. J.*, 2009, **15**, 13341–13347.

22. U. Y. Lee, Y. S. Youn, J. Park and E. S. Lee, *ACS Nano,* 2014, **12**, 12858–12865.

23. U. Y. Lee, Y. T. Oh, D. Kim and E. S. Lee, *Int. J. Pharm*., 2014, **471**, 166-172.

24. N. M. Oh, D. S. Kwag, S. Y. Park, K. T. Oh, Y. S. Youn and E. S. Lee, *Biomaterials*, 2012, **33**, 1884–1893.

25. M. E. Davis, Z. G. Chen and D. M. Shin, *Nat. Rev. Drug. Discov.*, 2008, **7**, 771–782.

26. D. Peer, J. M. Karp, S. Hong, O. C. Farokhzad, R. Margalit and R. Langer, *Nat. Nanotechnol.*, 2007, **2**, 751–760.

27. D. E. Dolmans, D. Fukumura and R. K. Jain, *Nat. Rev. Cancer*, 2003, **3**, 380–387.

Figure Captions

Fig. 1 Synthesis scheme of DOHA-*b*-poly(Lys-*g*-Ce6-*g*-mPEG-*g*-SA)

Fig. 2 (a) Schematic concept of AuNP with Ce6 sown in poly(ethylene glycol) forester (AuNP-P4). See the text for more details. (b) ^{1}H-NMR peaks of each polymer conjugate.

Fig. 3 TEM images of AuNP-P (bar size: 200 nm)

Fig. 4 (a) The emission spectra (at λ_{ex} 405 nm and λ_{em} 600-800 nm) of each AuNP-P (equivalent Ce6 10 μg/mL) or free Ce6 (10 μg/mL) in PBS (150 mM, pH 7.4). (b) The 9,10-dimethylanthracene (DMA) fluorescence change (at λ_{ex} 360 nm and λ_{em} 380-550 nm) of each AuNP-P (equivalent Ce6 10 μg/mL) or free Ce6 (10 μg/mL) in PBS (150 mM, pH 7.4). Singlet oxygen generation is indicated by change in the DMA fluorescence intensity (F_f-F_s).

Fig. 5 (a) Phototoxicities determined by a CCK-8 assay of KB cells treated with each AuNP-P (equivalent Ce6 1-10 μg/mL) or free Ce6 (1-10 μg/mL). All cells were irradiated for 10 min at a light intensity of 5.2 mW/cm^2 using a 670 nm laser source (n=7) (** $p < 0.01$ compared to free Ce6). (b) Cell viabilities of KB cells treated with each AuNP-P (10-100 μg/mL) without light illumination for 24 h (n=7).

Fig. 6 *In vivo* noninvasive photoluminescent imaging of each AuNP-P (*i.v.* dose: equivalent Ce6 0.5 mg/kg) or free Ce6 (*i.v.* dose: 2.5 mg/kg) injected intravenously into KB tumor-bearing nude mice. Fluorescence images were obtained at 1, 4, and 12 h post-injection. The tumor site is indicated by a dashed circle. (b) Fluorescence images of the sliced area of the *in vivo* tumor tissues extracted from KB tumor-bearing nude mice at 12 h post-injection of AuNP-P4 (*i.v.* dose: equivalent Ce6 0.5 mg/kg) or free Ce6 (*i.v.* dose: 2.5 mg/kg).

Fig. 7 (a) Relative tumor volume change (V/V_0, where V is the tumor volume at a given time, and V_0 is the initial tumor volume) of KB tumor-bearing nude mice locally irradiated at 12 h post-injection of each AuNP-P (*i.v.* dose: equivalent Ce6 0.5 mg/kg) or free Ce6 (*i.v.* dose: 2.5 mg/kg) or control (PBS) (n = 5) (b) Optical photographs of KB tumor-bearing nude mice. The tumor site is indicated by a dashed circle.

Table Captions

Table 1. Characterization of polymer conjugates

Samples		The degree of each segment (Ce6, mPEG, SA) substitution (DS) for DOHA-*b*-Poly(Lys)			Molecular weight of polymer conjugates		
Polymers	Code	Ce6	mPEG	SA	M_n [b]	M_w [c]	PDI [d]
		DS [a]	DS [a]	DS [a]	Unit: KDa		
DOHA-*b*-poly(Lys)	P1	—	—	—	3.1	4.3	1.39
DOHA-*b*-poly(Lys-*g*-SA)	P2	—	—	0.81	4.7	7.0	1.49
DOHA-*b*-poly(Lys-*g*-Ce6-*g*-SA)	P3	0.22	—	0.66	7.1	12.8	1.80
DOHA-*b*-poly(Lys-*g*-Ce6-*g*-mPEG-*g*-SA)	P4	0.22	0.19	0.52	14.5	27.7	1.91

[a] The degree of each segment (Ce6, mPEG, SA) substitution (DS) [defined as the number of each segment per repeating unit of DOHA-*b*-poly(Lys)] was estimated from ^{1}H-NMR.
Number average molecular weight (M_n)[b], weight average molecular weight (M_w)[c], and polydispersity index [PDI[d]: as calculated from the weight average molecular weight (M_w) divided by the number average molecular weight (M_n)] of polymer conjugates.

Table 2. Characterization of AuNP-P.

Samples	Components in AuNP-P	Ce6 content (wt%) in AuNP-P	Colloidal properties of AuNP-P	
			Size (average diameter)	Zeta-potential (mV)
AuNP-P2	AuNP + P2	—	51 nm	-28.9±2.2
AuNP-P3	AuNP + P3	21.8	56 nm	-31.9±0.8
AuNP-P4	AuNP + P4	12.9	75 nm	-16.5±1.6

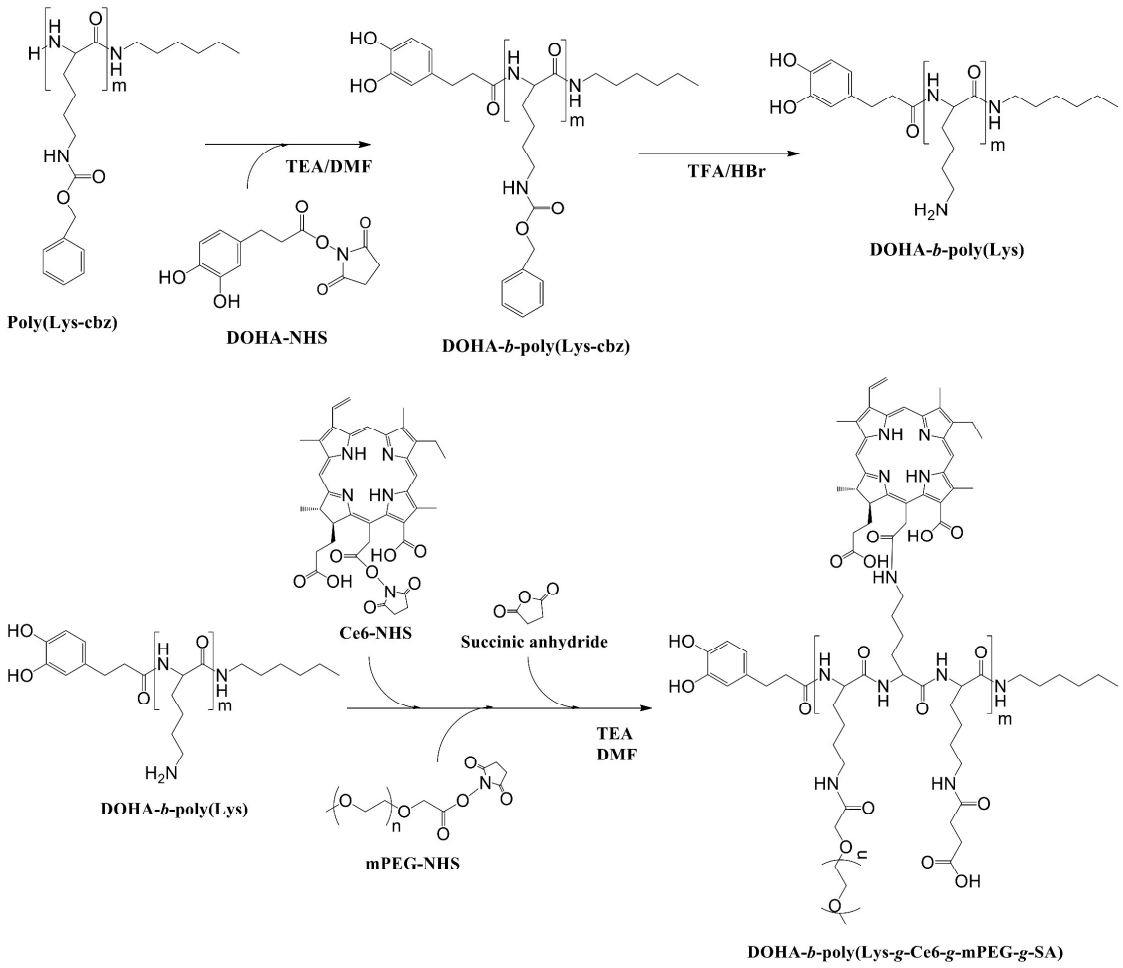

Fig. 1

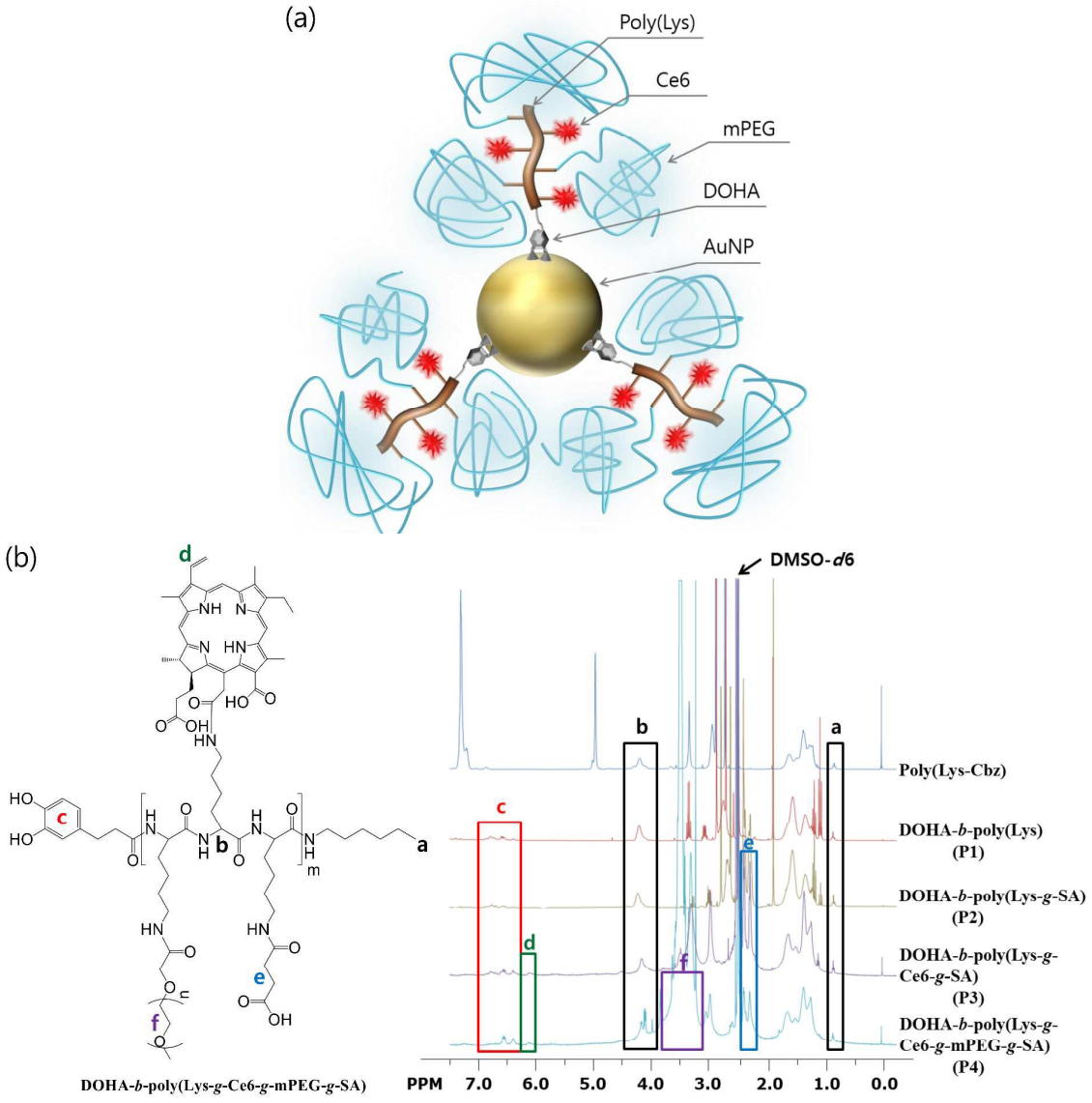

Fig. 2

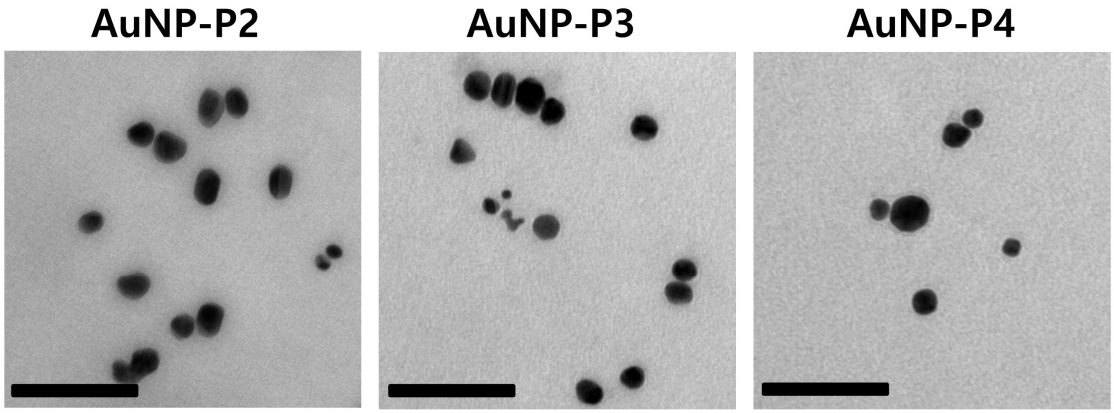

Fig. 3

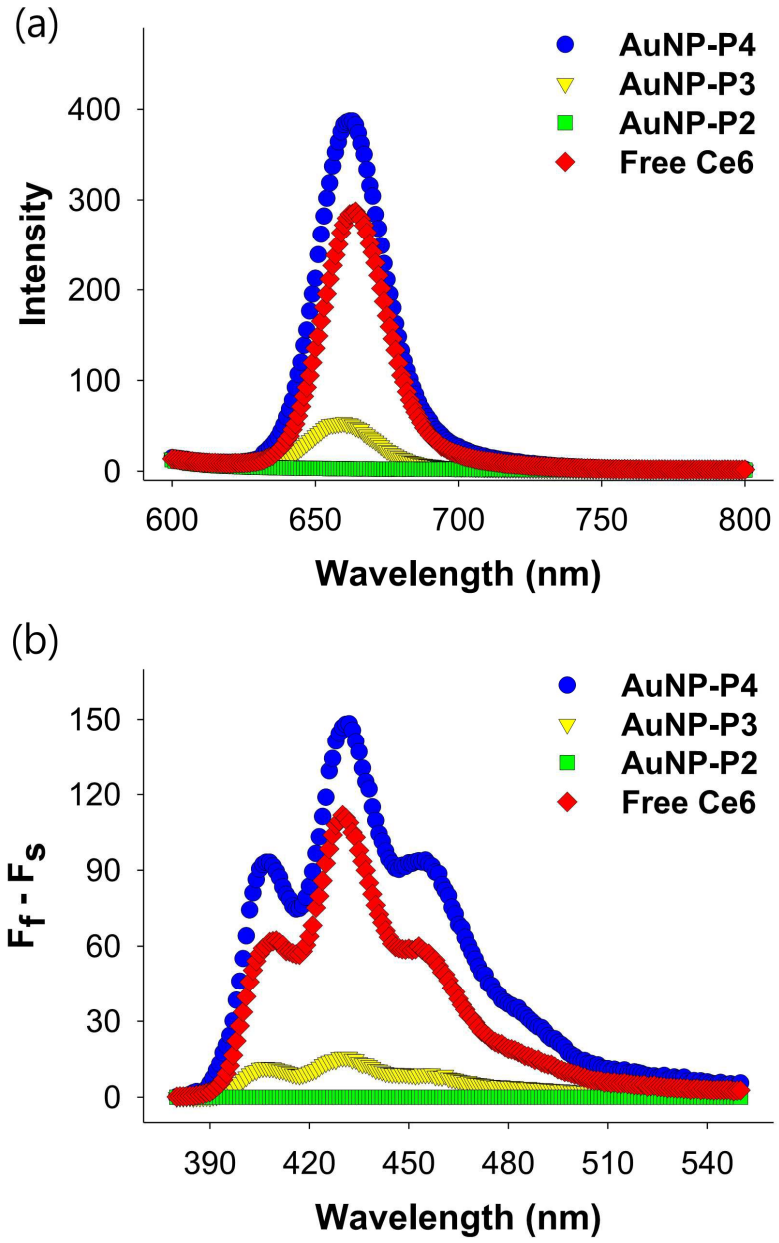

Fig.4

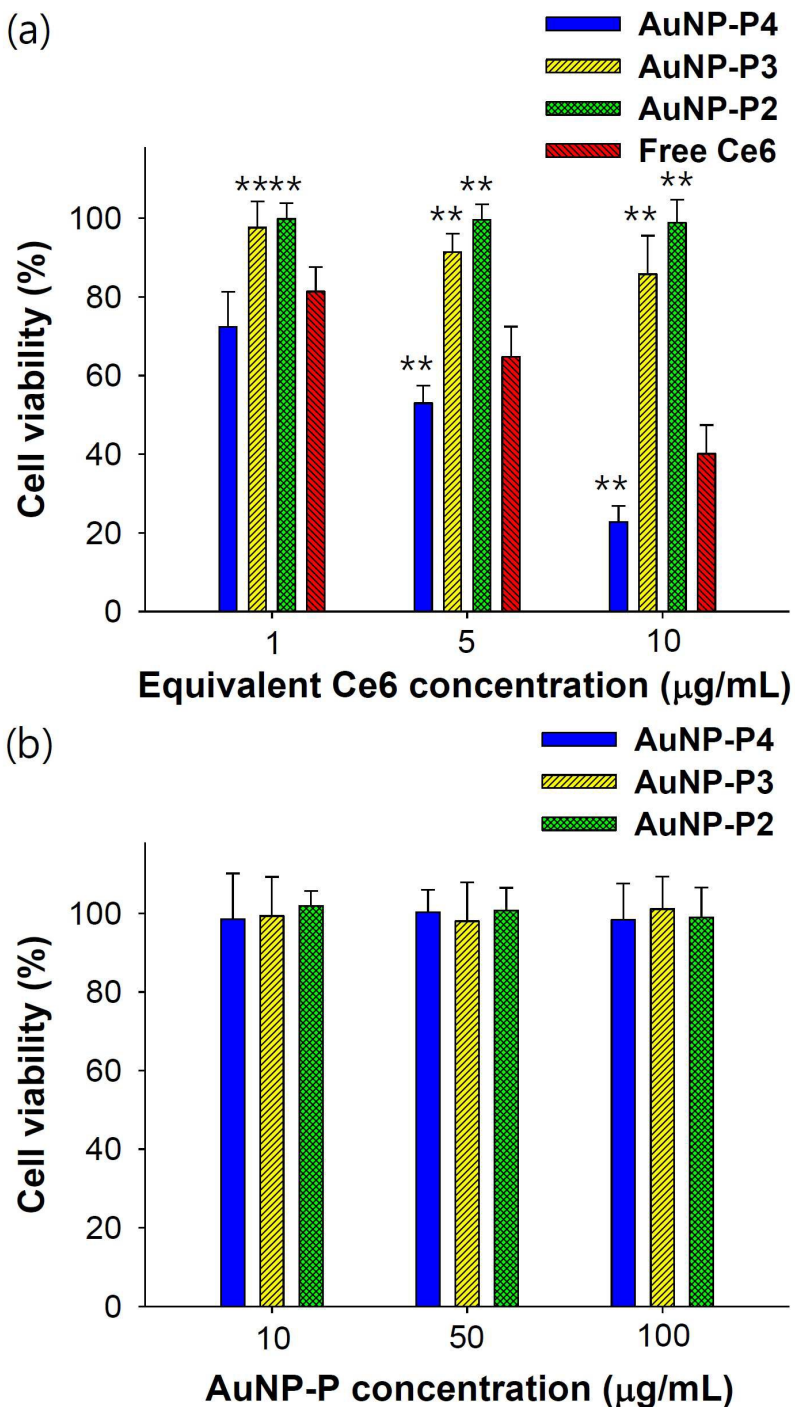

Fig. 5

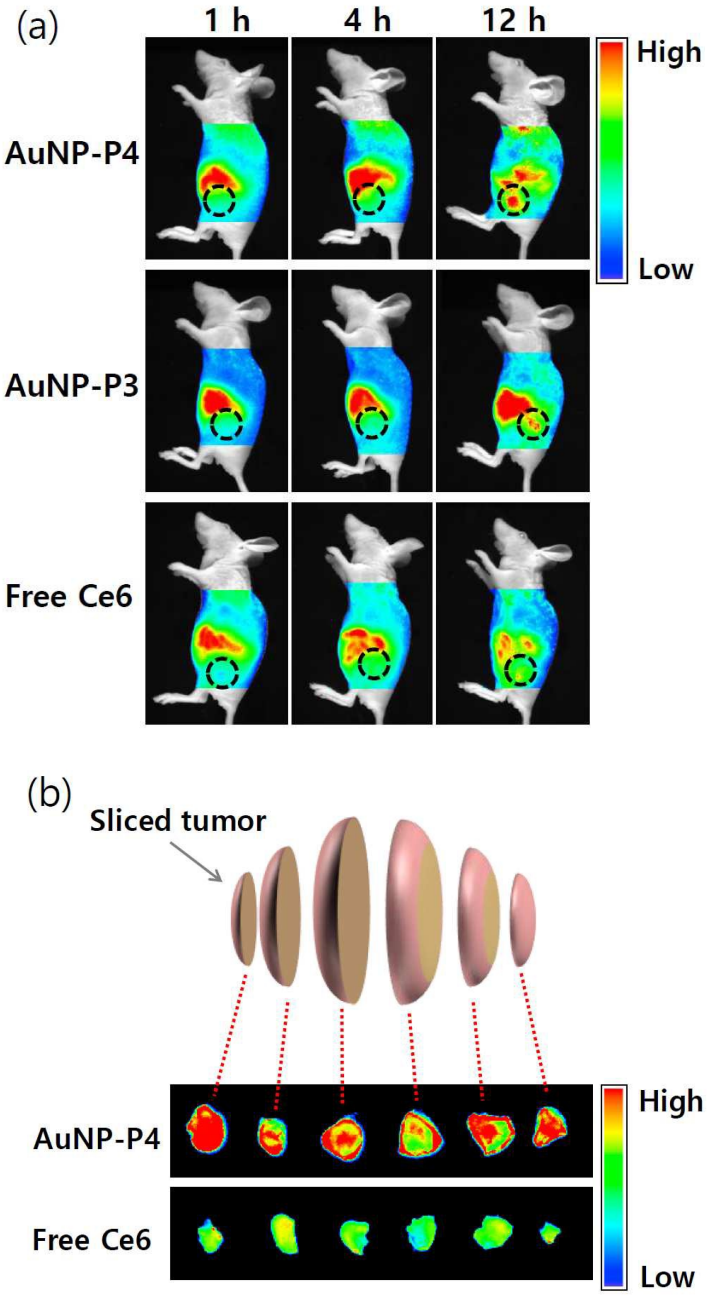

Fig. 6

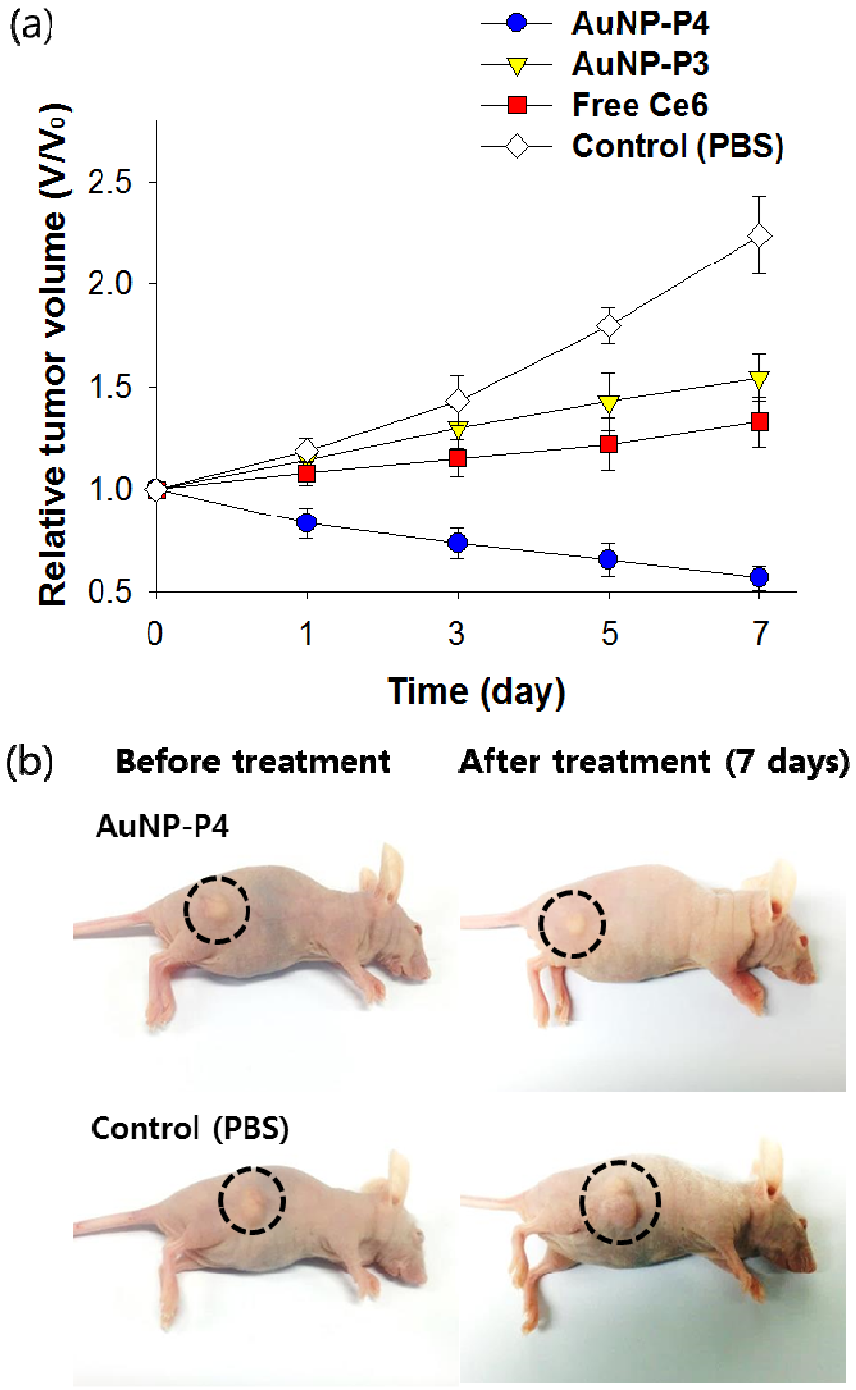

Fig. 7